

This document is confidential and is proprietary to the American Chemical Society and its authors. Do not copy or disclose without written permission. If you have received this item in error, notify the sender and delete all copies.

The headgroup (a)symmetry strongly determines the aggregation behavior of single-chain phenylene-modified bolalipids and their miscibility with classical phospholipids

Journal:	<i>Langmuir</i>
Manuscript ID:	la-2014-01160s.R2
Manuscript Type:	Article
Date Submitted by the Author:	n/a
Complete List of Authors:	Drescher, Simon; Martin-Luther-Universitaet Halle-Wittenberg, Institute of Pharmacy Lechner, Bob-Dan; Martin-Luther-Universitaet Halle-Wittenberg, Institute of Chemistry Garamus, Vasil; Helmholtz Zentrum Geesthacht (HZG), Almasy, Laszlo; Wigner Research Centre , Meister, Annette; Martin-Luther-Universitaet Halle-Wittenberg, Center for structure and dynamics of proteins (MZP) Blume, Alfred; Martin-Luther-Universitaet Halle-Wittenberg, Institute of Chemistry

SCHOLARONE™
Manuscripts

1
2
3
4
5
6
7
8
9
10
11
12
13
14
15
16
17
18
19
20
21
22
23
24
25
26
27
28
29
30
31
32
33
34
35
36
37
38
39
40
41
42
43
44
45
46
47
48
49
50
51
52
53
54
55
56
57
58
59
60

The headgroup (a)symmetry strongly determines the aggregation behavior of single-chain phenylene-modified bolalipids and their miscibility with classical phospholipids

Simon Drescher,^{†} Bob-Dan Lechner,[‡] Vasil M. Garamus,[¶] László Almásy,[§] Annette Meister,[#] Alfred Blume[‡]*

[†] Institute of Pharmacy, Martin-Luther-Universitaet (MLU) Halle-Wittenberg, Wolfgang-Langenbeck-Str. 4, 06120 Halle (Saale), Germany; [‡] Institute of Chemistry, MLU Halle-Wittenberg, von-Danckelmann-Platz 4, 06120 Halle (Saale), Germany; [¶] Helmholtz-Zentrum Geesthacht (HZG), Max-Planck-Str. 1, 21502 Geesthacht, Germany; [§] Wigner Research Centre for Physics, Budapest 1121 Konkoly Thege út 29, Hungary; [#] Center for structure and dynamics of proteins (MZP), MLU Halle-Wittenberg, Biocenter, Weinbergweg 22, 06120 Halle (Saale), Germany.

KEYWORDS

Bolalipids, Phospholipids, Aggregation Behavior, Self-Assembly, Mixing Behavior, Nanofibers, Micelles

ABSTRACT

In the present work, we describe the synthesis of two single-chain phenylene-modified bolalipids, namely PC-C17pPhC17-PC and PC-C17pPhC17-OH, with either symmetrical (phosphocholine) or asymmetrical (phosphocholine and hydroxyl) headgroups using a Sonogashira cross coupling reaction as key-step. The temperature-dependent aggregation behavior of both bolalipids in aqueous suspension was studied using transmission electron microscopy (TEM), differential scanning calorimetry (DSC), Fourier-transform infrared (FTIR) spectroscopy, small angle neutron scattering (SANS), and X-ray scattering. We show that different headgroup symmetries lead to a change in the aggregation behavior: Whereas PC-C17pPhC17-PC forms nanofibers with a diameter of 5.7 nm that transform into small ellipsoidal micelles at 23 °C, the PC-C17pPhC17-OH self-assembles into lamellae with bolalipid molecules in an antiparallel orientation up to high temperatures. Furthermore, the mixing behavior of both bolalipids with bilayer forming phospholipids (DPPC and DSPC) was studied by means of DSC and TEM. The aim was to stabilize bilayer membranes formed of phospholipids in order to improve these mixed lipid vesicles for drug delivery purposes. We show that the symmetrical PC-C17pPhC17-PC is miscible with DPPC and DSPC, however, closed lipid vesicles are not observed and elongated micelles and bilayer fragments are found instead. In contrast, the asymmetrical PC-C17pPhC17-OH shows no miscibility with phospholipids at all.

INTRODUCTION

Amphiphilic molecules with two hydrophilic headgroups attached to both ends of a long hydrocarbon spacer, consisting either of a single alkyl chain or two chains connected via a glycerol moiety, are called bolalipids.¹ Bolalipids can be found in the membrane lipids of certain species

1
2
3 of archaeobacteria where they are responsible for the outstanding stability of those membranes
4 against harsh external conditions, *e.g.*, very high temperature or low pH values.²⁻⁴ Chemically
5 pure representatives of naturally occurring symmetrical *double*-chain bolalipids and their
6 artificial analogues⁵⁻⁹ mostly form lamellar, sheet-like and vesicular aggregates in aqueous
7 suspension. On the other hand, symmetrical *single*-chain bolalipids composed of two large
8 phosphocholine (PC) headgroups attached to one alkyl chain, *e.g.* PC-C32-PC, self-assemble in
9 water into well-defined nanofibers, leading to an efficient gelation of the solvent.¹⁰ This self-
10 assembly process is exclusively driven by hydrophobic interactions of the long alkyl chain,
11 because the PC headgroups cannot form intermolecular hydrogen bonds. The nanofibers are
12 composed of bolalipid molecules that are arranged side by side but twisted relative to each other
13 due to the bulkiness of the PC headgroup in comparison to the small cross-sectional area of the
14 alkyl chain.¹⁰ The twisting leads to a helical superstructure of the nanofiber, which was proved
15 by high-resolution atomic force microscopy (AFM)¹¹ and coarse-grained off-lattice Monte Carlo
16 simulations.¹² Heating the hydrogel of a PC-C32-PC suspension above a distinct temperature
17 leads to the reversible transformation of the nanofibers into small spherical micelles and the gel
18 character is lost.¹⁰

19
20
21
22
23
24
25
26
27
28
29
30
31
32
33
34
35
36
37
38
39
40
41 By varying the chemical structure of these single-chain bolalipids the aggregation properties
42 can be influenced and controlled in a desired way. To achieve this intention, two types of
43 structural modifications are conceivable: (i) changes in the headgroup region and (ii) variations
44 within the alkyl spacer chain.¹³ For instance, the shortening of the alkyl chain leads to a decrease
45 of the fiber-micelle-transition and, hence, the gel-sol-conversion temperature.¹⁴ Moreover, since
46 the self-assembly of PC-C32-PC in aqueous suspensions is exclusively driven by van-der-Waals
47 interactions of the long alkyl chain, perturbations, such as the insertion of hetero atoms,¹⁵
48
49
50
51
52
53
54
55
56
57
58
59
60

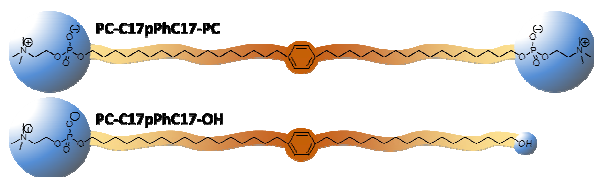
1
2
3 acetylene groups and methyl branches¹³ within the spacer chain result in a pronounced
4 destabilization of the fiber aggregates. On the other hand, modifications in the headgroup region
5
6 can be obtained, *e.g.*, by the reduction of the space requirement of the headgroup by a stepwise
7
8 replacement of methyl moieties. This leads to a series of phosphodimethylethanolamines
9
10 (Me₂PE-C_n-Me₂PE), which self-assemble into nanofibers¹⁶ or square lamellae,¹⁷ and the
11
12 phosphomonomethylethanolamine MePE-C32-MePE that forms monolayer-like structures.¹⁸
13
14
15

16
17 A further way of modifications that induces changes in aggregation properties is the intro-
18
19 duction of headgroup asymmetry, *i.e.*, the coupling of two headgroups of different size to the
20
21 same alkyl chain. This asymmetry leads to two different orientations of the bolalipids in lamellar
22
23 structures, either parallel or antiparallel. A parallel orientation of the bolalipids provokes the
24
25 formation of rods, nanotubes¹⁹⁻²¹ or nanotapes²² with, *e.g.*, a different curvature of the inner and
26
27 outer surface of the nanotube. On the other hand, an antiparallel (interdigitated) orientation of the
28
29 bolalipid results in the formation of monolayer-like aggregates.^{20,23} Recently, we investigated the
30
31 lyotropic behavior of DMAPPC-C32-OH,²⁴ an asymmetrical bolalipid bearing a large 2-(di-
32
33 methylaminopropyl)-PC (DMAPPC) headgroup and a small hydroxy moiety attached to a C32-
34
35 alkyl chain. This bolalipid self-assembles into short elongated micelles or lamellar structures,
36
37 depending on the protonation state.
38
39
40
41
42

43
44 Another promising property of bolalipids is that they can be inserted in a stretched
45
46 conformation into phospholipid bilayer membranes, leading to a stabilization of these phospho-
47
48 lipid vesicles. This stabilizing approach was adopted from naturally occurring archaeobacterial
49
50 membrane lipids^{4,25,26} and its applicability to drug delivery systems for pharmaceutical purposes
51
52 was confirmed for a variety of natural and artificial bolalipids.²⁷⁻³⁴
53
54

55
56 In our study we combine both, alkyl chain modifications and the introduction of headgroup
57
58
59
60

1
2
3 asymmetry. At first, we synthesized two novel single-chain bolalipids, namely PC-C17pPhC17-
4 PC and PC-C17pPhC17-OH. Both bolalipids are composed of a central para-substituted phenyl
5 ring within the alkyl chain and either two PCs headgroups (*symmetrical*) or a PC and hydroxy
6 ring within the alkyl chain and either two PCs headgroups (*symmetrical*) or a PC and hydroxy
7 ring within the alkyl chain and either two PCs headgroups (*symmetrical*) or a PC and hydroxy
8 ring within the alkyl chain and either two PCs headgroups (*symmetrical*) or a PC and hydroxy
9 ring within the alkyl chain and either two PCs headgroups (*symmetrical*) or a PC and hydroxy
10 ring within the alkyl chain and either two PCs headgroups (*symmetrical*) or a PC and hydroxy
11 (*asymmetrical*) headgroup (see Figure 1).



12
13
14
15
16
17
18
19
20 **Figure 1.** Chemical structure and schematic representation of single-chain phenylene-modified
21 bolalipids PC-C17pPhC17-PC and PC-C17pPhC17-OH investigated in this work.

22
23
24 Secondly, the temperature-dependent aggregation behavior in aqueous suspension of the
25 symmetrical bolalipid is compared to the self-assembly properties of its asymmetrical
26 counterpart using differential scanning calorimetry (DSC), Fourier-transform infrared (FTIR)
27 spectroscopy, transmission electron microscopy (TEM), small angle neutron scattering (SANS),
28 and X-ray scattering. Thirdly, we investigated the miscibility of the novel bolalipids with bilayer
29 forming 1,2-dipalmitoyl-*sn*-glycero-3-phosphocholine (DPPC) and 1,2-distearyl-*sn*-glycero-3-
30 phosphocholine (DSPC) by means of DSC and TEM. We will show that both, the alkyl chain
31 modification and the headgroup asymmetry of the bolalipids, have a great impact on the
32 aggregation behavior and also the miscibility with classical phospholipids.
33
34
35
36
37
38
39
40
41
42
43
44
45

46 EXPERIMENTAL SECTION

47 48 49 **Chemicals.**

50
51 1,2-Dipalmitoyl-*sn*-glycero-3-phosphocholine (DPPC) and 1,2-distearyl-*sn*-glycero-3-phospho-
52 choline (DSPC) were purchased from Lipoid KG (Ludwigshafen, Germany).
53
54
55

56 **Syntheses.**

1
2
3 The synthetic procedures and the analytical data of the substances are described in detail in the
4 Supporting Information (SI).
5
6

7 8 **Methods.**

9
10 *Sample preparation.* The appropriate amount of the bolalipid was suspended in H₂O (MilliQ)
11 and D₂O (Sigma Aldrich), respectively. Homogeneous suspensions were obtained by heating to
12 90 °C and vortexing. Binary lipid mixtures were prepared from lipid stock solutions in
13 CHCl₃/MeOH (2/1, v/v) as solvent by mixing appropriate volumes of the stock solutions.
14
15 Afterwards, the organic solvent was removed in a stream of N₂. The resulting lipid films were
16 kept in an evacuated flask for 24 h to remove residual traces of solvent. The suspensions were
17 then prepared by adding a certain volume of aqueous phosphate buffer (10 mM, pH = 7.4) to
18 obtain a total lipid concentration of 3 mM. The samples were vigorously vortexed for 30 min at
19 60 °C to obtain a homogeneous suspension.
20
21
22
23
24
25
26
27
28
29
30

31
32 *Differential Scanning Calorimetry (DSC).* DSC measurements were performed using a
33 MicroCal VP-DSC differential scanning calorimeter (MicroCal Inc. Northampton, MA, USA).
34 Before the measurements, the sample suspension and the water (or phosphate buffer) reference
35 were degassed under vacuum while stirring. A heating rate of 20 K h⁻¹ was used, and the
36 measurements were performed in the temperature interval from 2 °C to 95 °C. To check the
37 reproducibility, three consecutive scans were recorded for the sample. The water-water (buffer-
38 buffer) baseline was subtracted from the thermogram of the sample, and the DSC scans were
39 evaluated using MicroCal Origin 8.0 software.
40
41
42
43
44
45
46
47
48
49

50
51 *Transmission Electron Microscopy (TEM).* The negative stained samples were prepared by
52 spreading 5 μL of the bolalipid suspension ($c = 0.05 \text{ mg mL}^{-1}$) onto a copper grid coated with a
53 Formvar film. After 1 min, excess liquid was blotted off with filter paper and 5 μL of 1%
54
55
56
57
58
59
60

1
2
3 aqueous uranyl acetate solution were placed onto the grid and drained off after 1 min. Specimens
4 prepared below ambient temperature ($T = 5\text{ }^{\circ}\text{C}$) were dried for 2 days at $5\text{ }^{\circ}\text{C}$ and kept in an
5 exsiccator at ambient temperature. Specimens prepared in a modified drying oven above ambient
6 temperature were dried for 1 h at the appropriate temperature and kept in an exsiccator at
7 ambient temperature. All specimens were examined with a Zeiss EM 900 transmission electron
8 microscope (Carl Zeiss Microscopy GmbH, Oberkochen, Germany).

9
10
11
12
13
14
15
16
17 *Fourier-transform Infrared Spectroscopy (FTIR).* Infrared spectra were collected on a Bruker
18 Vector 22 Fourier transform spectrometer with DTGS detector operating at 2 cm^{-1} resolution.
19 Sample ($c = 50\text{ mg mL}^{-1}$ in D_2O) were placed between two CaF_2 windows, separated by a $56\text{ }\mu\text{m}$
20 spacer. IR spectra were recorded in steps of 2 K in the temperature range from $9\text{ }^{\circ}\text{C}$ to $75\text{ }^{\circ}\text{C}$.
21 After an equilibration time of 8 min, 64 scans were recorded and accumulated. The corre-
22 sponding spectra of the solvent (D_2O) were subtracted from the sample spectra using the OPUS
23 software supplied by Bruker.
24
25
26
27
28
29
30
31
32

33
34 *Small angle neutron scattering (SANS).* SANS measurements were performed on the Yellow
35 Submarine instrument at the BNC in Budapest (Hungary).³⁵ The overall q -range was from
36 0.03 nm^{-1} to 1.0 nm^{-1} . The samples were filled in Hellma quartz cells of 2 mm path length and
37 placed in a thermostated holder kept with accuracy $\pm 0.5\text{ }^{\circ}\text{C}$. The raw scattering patterns were
38 corrected for sample transmission, room background, and sample cell scattering. The two-
39 dimensional scattering patterns were azimuthally averaged, converted to an absolute scale and
40 corrected for detector efficiency dividing by the incoherent scattering spectra of 1 mm thick pure
41 water. The scattering from D_2O was subtracted as the background.
42
43
44
45
46
47
48
49
50
51
52

53 *X-ray scattering.* Powder patterns were measured in transmission with a stationary linear
54 position sensitive detector ($2\theta = 0\text{--}44^{\circ}$) on a stage including primary Ge(111) monochromator
55
56
57
58
59
60

1
2
3 and high temperature attachment (STOE & CIE, Darmstadt, Germany). The bolalipid samples
4 (50 wt.% H₂O) were sealed in glass capillaries (diameter 1.5 mm). CuK_{α1} ($\lambda = 0.154051$ nm)
5 radiation was used, and the scattering was corrected with respect to a capillary filled with H₂O
6 ($I_{norm} = I_{sample}/I_{cap}$). The X-ray patterns were combined in a single contour diagram to
7 continuously present the scattered intensity from the SAXS to the WAXS region ($2\theta = 0-44^\circ$,
8 $s = 0-4.7$ nm⁻¹) between -30 °C and 135 °C in steps of 2 K. The heating rate was $1/15$ K min⁻¹
9 (5 min equilibration, 10 min exposition for each pattern) for the applied temperature protocol.
10
11
12
13
14
15
16
17
18
19

20 RESULTS AND DISCUSSION

21 Syntheses of bolalipids

22
23
24 For the synthesis of the symmetrical bolalipid we converted the phenylene-modified 1, ω -diol,
25 which was synthesized using the bis-Sonogashira cross-coupling reaction described previously,³⁶
26 into the PC-C17pPhC17-PC by established phosphorylation and quarternisation reactions (see
27 SI, Scheme S1, left panel). For the synthesis of the asymmetrical PC-C17pPhC17-OH we used a
28 similar Sonogashira cross-coupling reaction as key step and HO-C15pAcPh-Br and Ac-C15-OBn
29 as starting materials. The Ac-C15-OBn can be prepared in three steps from THPO-C15-Br¹⁴ as
30 detailed in the SI. The Sonogashira cross-coupling of HO-C15pAcPh-Br with Ac-C15-OBn was
31 carried out under comparable conditions as described for the bis-coupling reaction,³⁶ and the
32 HO-C15pAcPhAcC15-OBn was obtained in 61% yield after chromatographic purification. This
33 mono-protected diol was then transformed into the bolalipid PC-C15pAcPhAcC15-OBn by
34 phosphorylation and quarternisation reaction.¹⁴ The final step combined the cleavage of the Bn
35 protecting group and the hydrogenation of the triple bonds, resulting in the formation of the
36 asymmetrical bolalipid PC-C17pPhC17-OH (Scheme S1, right panel).
37
38
39
40
41
42
43
44
45
46
47
48
49
50
51
52
53
54
55
56
57
58
59
60

1
2
3 The stepwise performed Sonogashira cross-coupling reaction of dibromo benzene derivatives
4 with various, orthogonally protected alkynols is a promising method for the preparation of
5 phenylene-modified 1, ω -diols and, in continuation, asymmetrical bolaphospholipids. Hence, this
6 synthetic pathway is a valuable amendment to the synthesis of phenylene-modified diols using
7 the Grignard homo-coupling reactions published previously.³⁷
8
9

16 **Temperature-dependent aggregation behavior of pure bolalipids in aqueous suspension**

18 Symmetrical single-chain bolalipids without chain modifications mostly aggregate in water into
19 long, flexible nanofibers resulting in the formation of a transparent hydrogel. A temperature
20 increase leads to the transformation of the fibers into small spherical micelles and the
21 liquefaction of the gel. This transition is reversible and it can be monitored by DSC, TEM, and
22 FTIR.¹⁰ In the DSC thermogram of, *e.g.*, PC-C32-PC two endothermic transitions (T_m) were
23 observed, the first one at 48.7 °C that is attributed to the breakdown of the nanofibers and the
24 second one at about 73 °C representing a transition between two different types of micelles.¹⁴
25
26

35 *TEM:*

37 When suspended in water, the bolalipid PC-C17pPhC17-PC ($c = 1 \text{ mg mL}^{-1}$) forms a
38 transparent hydrogel after storage in the refrigerator at 4 °C (see Figure S1). This behavior
39 indicates a self-assembly of PC-C17pPhC17-PC into nanofibers as observed for similar
40 phenylene-free bolalipids. However, the hydrogel of PC-C17pPhC17-PC is not as stable as
41 hydrogels formed of, *e.g.*, PC-C32-PC. In contrast, the asymmetrical bolalipid PC-C17pPhC17-
42 OH forms no hydrogel. Instead, the formation of an opalescent suspension after several heating
43 and vortexing cycles was observed (see Figure S1). To visualize the structures of aggregates
44 formed in the aqueous suspensions at 20 °C TEM images were obtained from both negatively
45 stained samples (Figure 2).
46
47
48
49
50
51
52
53
54
55
56
57
58
59
60

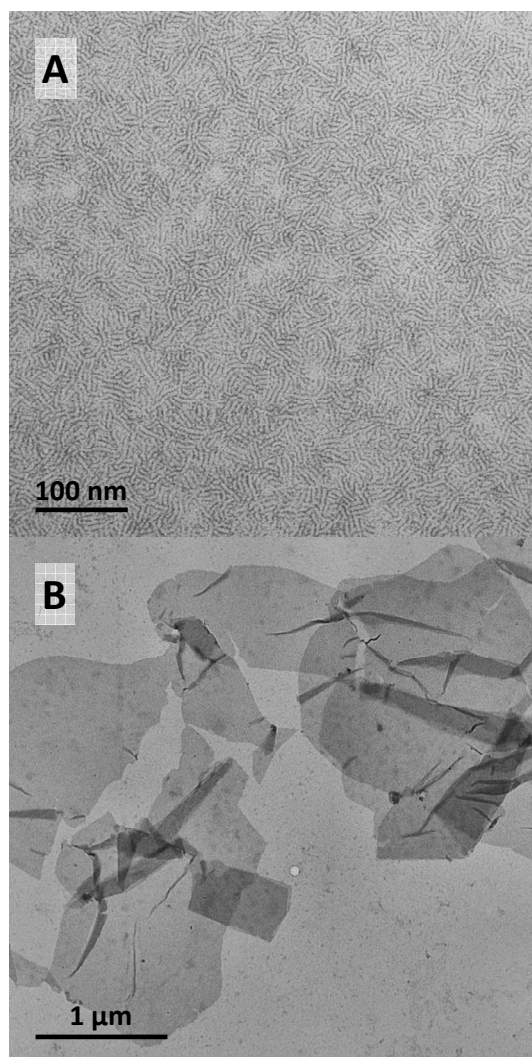


Figure 2. TEM images of aqueous suspension ($c = 0.05 \text{ mg mL}^{-1}$) of (A) PC-C17pPhC17-PC and (B) PC-C17pPhC17-OH. The samples were prepared at 20 °C and stained with uranyl acetate.

The TEM image of the symmetrical PC-C17pPC17-PC (Figure 2A) shows the presence of densely packed nanofibers. The thickness of the nanofibers is 5–6 nm, which roughly corresponds to the length of the bola molecule. A similar symmetrical bolalipid, namely PC-C16pPhC16-PC³⁷ with a slightly shorter alkyl chain (two methylene units) compared to the bolalipid described here, shows the formation of small elongated micelles in aqueous suspension at room temperature. These micelles have a size between 8 nm and 18 nm in length and 3–4 nm in width. However, the formation of nanofibers and, hence, a gelation of the solvent were not

observed for the PC-C16pPhC16-PC sample. This indicates that the tendency to form fibrous aggregates depends critically on the over-all alkyl chain length of the phenylene-modified bolalipids: The shortening of the alkyl chain by two methylene units is sufficient to reduce the van-der-Waals contacts of neighboring alkyl chains in such a manner that the formation of long nanofibers is not possible.

In contrast to the symmetrical bolalipid, the TEM image of the asymmetrical counterpart PC-C17pPhC17-OH (Figure 2B) shows the presence of large lamellar structures. These sheet-like aggregates that in the TEM image appear folded and partly disrupted have a size of about several micrometers. The folding is due to the drying process during the EM sample preparation. In consequence, the aggregation behavior of phenylene-modified bolalipids can be tuned by simple changes in the headgroup asymmetry, *i.e.*, the replacement of one PC headgroup of the bolalipid by a small hydroxy moiety. A comparable behavior was observed previously for phenylene-free bolalipids with a larger difference in the size of the two headgroups attached at one alkyl chain.²⁴

DSC and FTIR:

To investigate the temperature-dependent aggregation behavior of both bolalipids in aqueous suspension, DSC and FTIR measurements were carried out (Figure 3).

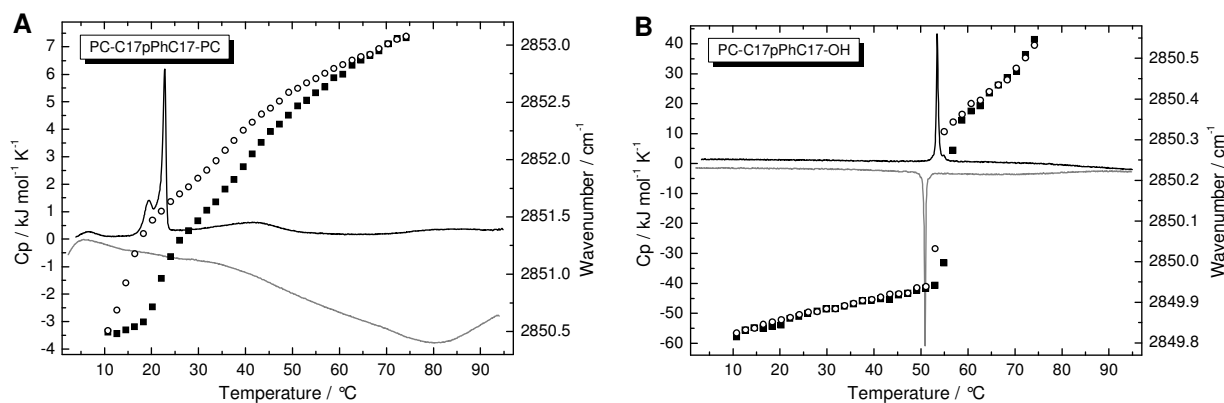


Figure 3. DSC data (solid lines, $c = 1 \text{ mg mL}^{-1}$ in H_2O , heating: black, cooling: grey) and FTIR spectroscopic data (symmetric methylene stretching vibration, scattered data, $c = 50 \text{ mg mL}^{-1}$ in

1
2
3 D₂O, heating: filled squares, cooling: open circles) of (A) PC-C17pPhC17-PC and (B) PC-
4 C17pPhC17-OH.
5
6

7 The DSC heating curve of the PC-C17pPhC17-PC shows three endothermic peaks (Figure
8 3A): a very small peak at 6.6 °C, a second one at 22.8 °C that probably corresponds to a fiber-
9 micelle-transition, and a third very broad peak between 40–42 °C, which can be attributed to a
10 transition between two different types of micelles. In contrast, the similar bolalipid PC-
11 C16pPhC16-PC showed only the formation of small micelles at room temperature and no
12 transition was observed in the DSC in the temperature range between 2–95 °C (see Figure
13 S2).^{13,37} The corresponding cooling curve of the PC-C17pPhC17-PC suspension shows no
14 transition peaks, which is an indication for a hindered reformation of the fibrous aggregates on
15 the time scale of the cooling process. As mentioned above, for the formation of the nanofibers
16 the sample has to be kept at 4 °C for prolonged periods of time. Since the DSC scans of
17 suspensions of the unmodified PC-C32-PC¹⁴ and PC-C34-PC¹¹ show a very cooperative fiber-
18 micelle-transition at 48.7 °C and 56.5 °C, the decreased transition temperature for PC-
19 C17pPhC17-PC reflects the strong influence of the phenyl ring in the middle part of the alkyl
20 chain on the van-der-Waals interactions between neighboring alkyl chains and the perturbation of
21 optimal chain packing necessary for the formation of stable nanofibers. This phenomenon was
22 also described for other alkyl chain modifications, such as the insertion of sulfur atoms,¹⁵ acety-
23 lene groups, and methyl branches.¹³ The fact that the shorter chain analogue PC-C16pPhC16-PC
24 forms only micelles reveals the existence of a critical length for the unmodified alkyl chain,
25 below which a formation of nanofibers is not possible any more. To investigate the structure of
26 aggregates formed in aqueous suspension below and above T_m of PC-C17pPhC17-PC, samples
27 for TEM were also prepared at 4 °C and 35 °C, respectively. The TEM images (see Figures S3,
28 S4) show the presence of flexible nanofibers below T_m and worm-like micelles above T_m . These
29
30
31
32
33
34
35
36
37
38
39
40
41
42
43
44
45
46
47
48
49
50
51
52
53
54
55
56
57
58
59
60

micelles are comparable to the aggregates formed of PC-C16pPhC16-PC at room temperature.³⁷

In contrast to the symmetrical bolalipid PC-C17pPhC17-PC, the DSC heating curve of the asymmetrical PC-C17pPhC17-OH shows only one endothermic and very cooperative transition at 53.4 °C in the temperature range up to 95 °C (Figure 3B). The corresponding cooling curve reveals the same peak with a small hysteresis of 2.5 K.

To obtain information on the chain conformation of the bolalipid molecules inside the formed aggregates, IR spectra of suspensions of both bolalipids ($c = 50 \text{ mg mL}^{-1}$ in D_2O) were recorded in the temperature range between 9–75 °C. The wavenumbers of the symmetric ($\nu_s\text{CH}_2$) and antisymmetric ($\nu_{as}\text{CH}_2$) methylene stretching vibrational bands provide information about the conformational order of the alkyl chain.^{38,39} The temperature dependency of the wavenumbers of both methylene stretching vibrational bands of PC-C17pPhC17-PC and PC-C17pPhC17-OH is depicted in Figure 3, and in the SI in Figures S5, S6.

For the symmetrical PC-C17pPhC17-PC, the frequency of the bands at low temperatures are at 2850.5 cm^{-1} and 2919.8 cm^{-1} for $\nu_s\text{CH}_2$ (Figure 3A) and $\nu_{as}\text{CH}_2$ (Figure S5), respectively, and indicate ordered alkyl chains in all-*trans* conformation. The frequencies are slightly higher compared to the CH_2 -stretching frequencies of the unmodified PC-C32-PC (2849.6 cm^{-1} and 2918.6 cm^{-1})¹⁰ due to the reduced van-der-Waals contacts of the phenylene-modified alkyl chains and/or to the overall shorter alkyl chains of PC-C17pPhC17-PC compared to PC-C32-PC. The wavenumber of both bands increases to 2853.1 cm^{-1} ($\nu_s\text{CH}_2$) and 2924.3 cm^{-1} ($\nu_{as}\text{CH}_2$) at 75 °C. This increase in wavenumber, which is most pronounced in the temperature range around T_m (at 23 °C), is attributed to an increased amount of *gauche* conformers and, hence, a more flexible alkyl chain. The cooling curve shows nearly the same pattern for both stretching vibrational bands except a hysteresis of about 5 K indicating a delayed reformation of the ordered fibrous

1
2
3 structures. This hysteresis is not visible in the DSC cooling scan due to the higher bolalipid
4 concentration in the DSC experiment compared to the samples used for FTIR, as the kinetics for
5 reformation of the nanofibers from micelles is, of course, concentration dependent.
6
7
8
9

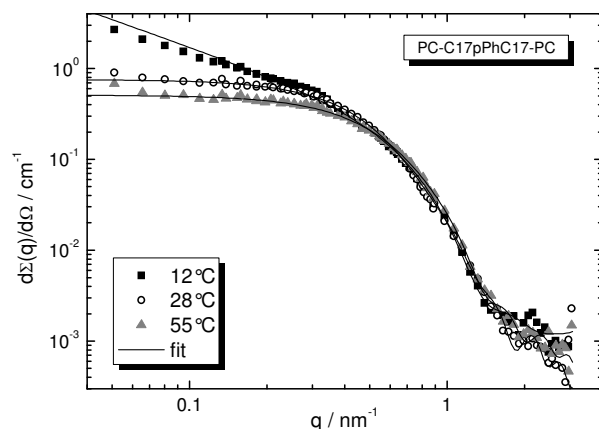
10 For the asymmetrical PC-C17pPhC17-OH the wavenumbers of both methylene stretching
11 vibrational bands occur at 2849.8 cm^{-1} ($\nu_s\text{CH}_2$, Figure 3B) and 2917.0 cm^{-1} ($\nu_{as}\text{CH}_2$, see Figure
12 S6). These values are slightly lower compared to the νCH_2 -bands of the symmetrical counterpart
13 indicating more highly ordered alkyl chains. During heating, the wavenumbers of both bands
14 increase to 2850.4 cm^{-1} ($\nu_s\text{CH}_2$) and 2919.0 cm^{-1} ($\nu_{as}\text{CH}_2$) above T_m ($53\text{ }^\circ\text{C}$). Both frequency
15 values indicate that the alkyl chain is still in an all-*trans* conformation, *i.e.*, no “melting” of the
16 alkyl chain occurs at this temperature.
17
18
19
20
21
22
23
24
25
26

27 To investigate the nature of this transition, the methylene scissoring vibrational band (δCH_2)
28 was analyzed. The temperature dependent spectra for both bolalipids are shown in the SI (see
29 Figures S7, S8): At low temperatures one observes a band at ca. 1471.5 cm^{-1} for the symmetrical
30 and 1472.1 cm^{-1} for the asymmetrical bolalipid. For both bolalipids the bands decrease in
31 intensity and shift to lower wavenumbers with increasing temperature. At the main transition
32 temperature, for PC-C17pPhC17-PC a shift to 1468.0 cm^{-1} is observed when the nanofibers
33 convert into micelles. For PC-C17pPhC17-OH the shift occurs to 1467.5 cm^{-1} . For the
34 asymmetrical bolalipid PC-C17pPhC17-OH this change in frequency is conceivably related to
35 different chain packing modes in the ordered lamellar phases. However, in contrast to previous
36 results found for the lamellar phase of an asymmetric phenylene-free bolalipid,²⁴ a splitting of
37 the methylene deformational band was not observed at low temperature indicating an ortho-
38 rhombic perpendicular packing of the alkyl chains.⁴⁰⁻⁴³ Obviously, the additional phenyl ring in
39 the middle part of the alkyl chain leads to some distortion and the alkyl chains cannot come in a
40
41
42
43
44
45
46
47
48
49
50
51
52
53
54
55
56
57
58
59
60

1
2
3 very close and highly ordered contact required for the appearance of this splitting. Nevertheless,
4
5 the change in frequency of the CH₂-stretching bands and the CH₂-deformation band indicates a
6
7
8 very cooperative change in chain packing at this temperature. It is conceivable that the chains
9
10 gain rotational freedom but are still in an all-*trans* conformation.
11

12 SANS and X-ray:

13
14
15 To get further insight into the structure of aggregates formed of both bolalipids, SANS and X-
16
17 ray scattering measurements were performed. At first, a suspension of the symmetrical PC-
18
19 C17pPhC17-PC ($c = 2 \text{ mg mL}^{-1}$ in D₂O) was investigated by SANS at different temperatures.
20
21 The scattering data and their fits are shown in Figure 4. The fits were performed using the IFT
22
23 method described before^{16,18,44,45} and they are in quite good agreement with the experimental
24
25 data. For fitting the scattering data obtained at 12 °C, the model of infinitely long cylinders was
26
27 used and for the fits of the scattering curves obtained at 28 °C and 55 °C spherical aggregates
28
29 were assumed. The results of the fits are provided in Table 1.
30
31
32
33



49 **Figure 4.** SANS data (symbols) and IFT fits (solid lines) of an aqueous suspension of PC-
50 C17pPhC17-PC ($c = 2 \text{ mg mL}^{-1}$ in D₂O) measured at different temperatures.
51
52
53
54
55
56
57
58
59
60

Table 1. SANS data obtained from IFT fits for aqueous suspensions of PC-C17pPhC17-PC in D₂O at different temperatures.^a Data for PC-C32-PC and PC-C36-PC are shown for comparison.

Bolalipid (concentration)	$T [^{\circ}\text{C}]$	Aggregate shape	D_{max} [nm]	M [g] or M_L [g cm ⁻¹]	N_{agg} [nm ⁻¹] or N_{agg} per micelle	R_g or $R_{\text{SC},g}$ [nm]	R [nm]
PC-C17pPhC17-PC ($c = 2 \text{ mg mL}^{-1}$)	12	fibers	6.5	$9.35 \cdot 10^{-14}$	6 ± 1	2.01 ± 0.02	2.84 ± 0.02
	28	micelles	11.0	$1.21 \cdot 10^{-19}$	79 ± 4	3.77 ± 0.05	4.87 ± 0.05
	55	micelles	10.0	$8.57 \cdot 10^{-20}$	56 ± 3	3.30 ± 0.02	4.26 ± 0.02
PC-C32-PC ¹⁶ ($c = 1 \text{ mg mL}^{-1}$)	25	fibers	4.5	$1.47 \cdot 10^{-13}$	10 ± 1	1.51 ± 0.02	2.14 ± 0.02
	60	micelles	7.5	$1.05 \cdot 10^{-19}$	77 ± 3	2.46 ± 0.02	3.18 ± 0.02
PC-C36-PC ¹⁷ ($c = 1 \text{ mg mL}^{-1}$)	25	fibers	5.5	$1.46 \cdot 10^{-13}$	10 ± 1	1.86 ± 0.02	2.63 ± 0.01
	70	micelles	7.5	$9.87 \cdot 10^{-20}$	77 ± 4	2.71 ± 0.02	3.50 ± 0.02

^a D_{max} : maximal size or cross-section of aggregate, M : mass, M_L : mass per unit length, N_{agg} : aggregation number, R_g : radius of gyration, $R_{\text{SC},g}$: radius of gyration of cross-section, R and R_{SC} are effective radius of aggregate or radius of cylindrical cross section in homogeneous approximation.

The results of the fits support the interpretation of the aggregate structure of PC-C17pPhC17-PC as fibers below and micelles above the main DSC transition peak. The mean diameter (d) of the bola fibers ($d = 5.7 \text{ nm}$) is in accordance with the one determined from TEM and corresponds roughly to the length of the bola molecule. If the additional phenyl ring in the middle part of the alkyl chain is set to a length of roughly 4 C-C bonds, PC-C17pPhC17-PC has an alkyl chain length equal to a C38-chain. Hence, the diameter of the PC-C17pPhC17-PC nanofiber fits well into the series of bola fibers composed of unmodified C32- (PC-C32-PC, $d = 4.3 \text{ nm}$; Table 1)¹⁶ and C36-bolalipid molecules (PC-C36-PC, $d = 5.3 \text{ nm}$).¹⁷ Modelling the scattering curves assuming stiff cylinders with an elliptical cross-section leads to values for the semi axes of $2.1 \pm 0.1 \text{ nm}$ and $3.4 \pm 0.1 \text{ nm}$ (axial ratio about 1.6, see Table S2). The PC-C17pPhC17-PC nanofibers have a lower aggregation number $N_{\text{agg}} \text{ nm}^{-1}$ compared to the unmodified bolalipids (6 vs. 10; see Table 1). It is obvious that the insertion of a phenyl ring in the middle part of the alkyl chain increases the space requirement (volume) of the alkyl chain as well as the whole bola molecule and, hence, decreases $N_{\text{agg}} \text{ nm}^{-1}$.

1
2
3 As mentioned before, small micellar aggregates are observed for the aqueous PC-
4 C17pPhC17-PC suspension at temperatures above T_m . At 28 °C we obtain a mean diameter of the
5 micelles of 9.7 nm and a N_{agg} (number of molecules per micelle) of 79. Modelling of the
6 scattering curves by ellipsoids of revolution yields values for the semi axes of $a = b = 3.2$ nm and
7 $c = 8.2$ nm (see Table S2). Compared to the unmodified bolalipids the mean diameter is slightly
8 larger, which is due to the additional phenyl ring within the alkyl chain and an over-all longer
9 alkyl chain, but the aggregation numbers are similar. Above the very broad DSC transition
10 between 40–42 °C, d and N_{agg} decrease to 8.5 nm and 56 due to a higher amount of *gauche*
11 conformers within the alkyl chain. This change in the aggregate size of two different types of
12 micelles was also found for aggregates formed of PC-C26-PC with an unmodified alkyl chain of
13 26 methylene units.¹⁸ However, the arrangement of the bolalipid molecules within these different
14 types of micellar aggregates remains still unclear at this time.

15
16
17
18
19
20
21
22
23
24
25
26
27
28
29
30
31
32 The suspension of the asymmetrical PC-C17pPhC17-OH was not investigated by SANS as
33 large lamellar aggregates are formed with highly ordered chains. X-ray diffraction measurements
34 at different temperatures were performed instead, to gain information about the molecular
35 packing and structural organization of the bolalipid molecules within the lamellar aggregates.
36
37
38
39
40
41
42
43
44
45
46
47
48
49
50
51
52
53
54
55
56
57
58
59
60
The results are shown in Figure 5 as a contour plot.

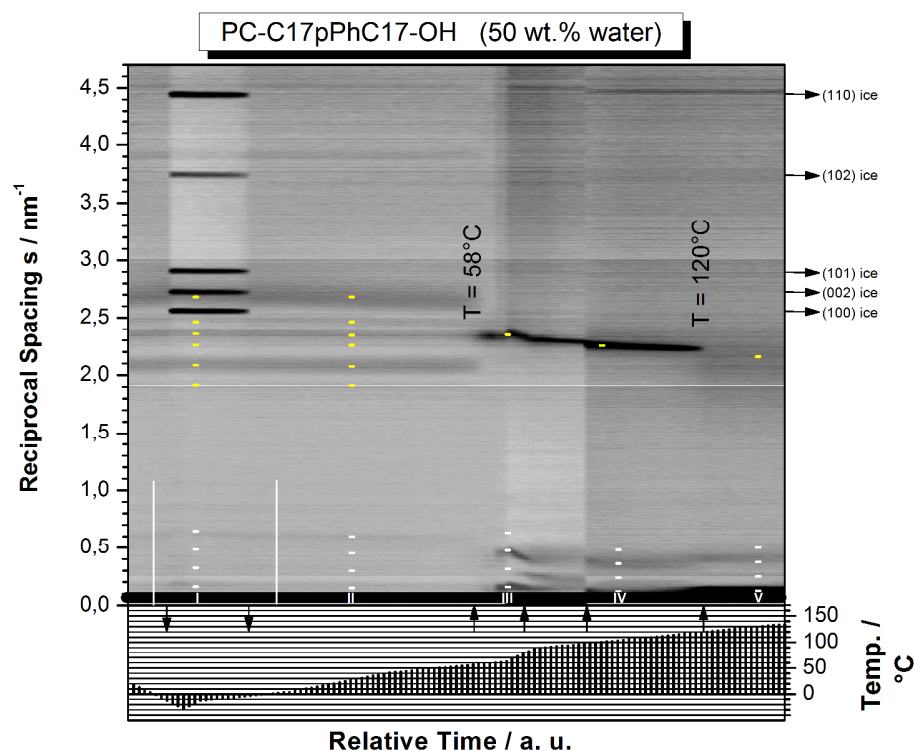
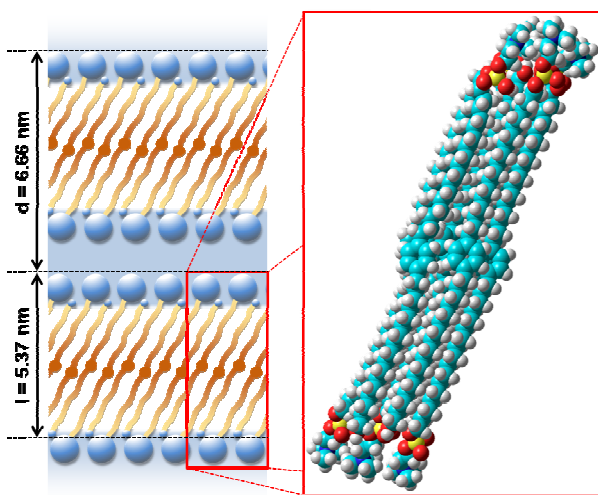


Figure 5. X-ray contour diagram of a 50 wt.% PC-C17pPhC17-OH sample in water. The scattering intensities are shown in the upper part as a function of reciprocal lattice spacing (*ordinate*) and temperature (*abscissa*). In the lower part the temperature course during the experiment is shown as a *ramp*. The two *arrows pointing down* indicate the onset of freezing and melting of water. In the temperature range between these arrows additional intense ice reflections are seen. The *arrows pointing upwards* indicate the transition temperatures of the bolalipid in the up and down scans. The intensities in the diagram have been scaled differently in the different temperature ranges, visible by the changes in gray scaling of the background intensity. Long spacings (different orders of the repeat distance, *white dashes*) and respective short spacings (fingerprint scattering due to the aliphatic chain packing, *yellow dashes*) belong together at the selected temperatures I–V: (I) $d = 6.21$ nm ($s = 0.161$ nm⁻¹, -18 °C), (II) $d = 6.66$ nm ($s = 0.150$ nm⁻¹, 20 °C), (III) $d = 6.32$ nm ($s = 0.158$ nm⁻¹, 70 °C), (IV) $d = 8.33$ nm ($s = 0.120$ nm⁻¹, 100 °C), (V) $d = 8.00$ nm ($s = 0.125$ nm⁻¹, 135 °C). Two light *vertical lines* are drawn at 0 °C to illustrate the super cooling of water.

At ambient temperature, up to 4 equidistant reflections in the small angle scattering (SAXS) region but with only very weak intensities are present (see also SI, Figure S9 and Table S3). Thus, the lamellar structures formed are only poorly ordered in the z -direction. The determined repeat distance (membrane thickness plus inter-lamellar water layer thickness) is $d = 6.66$ nm

1
2
3 and, hence, in the range of typical bolalipids^{17,24} forming monolayer lamellar structures.
4
5 Compare to the molecule length of about 6.2 nm, the observed repeat distance of 6.66 nm again
6
7 indicates an monolayer lamellar phase with interdigitated chains as observed before for the
8
9 bolalipid DMAPPC-C32-OH with unmodified chain but different headgroup²⁴ and for an
10
11 asymmetrical single-chain bolalipid with a shorter, unmodified alkyl chain (PC-C22-OH).⁴⁶
12
13 However, for the water layer a thickness of only 0.46 nm would result. This is unlikely, as the
14
15 PC headgroup is normally well hydrated. We therefore propose a tilting of the chains relative to
16
17 the layer normal (Figure 6). This tilting of the chains would also lead to a better packing of the
18
19 phenyl rings in the middle of the layer. Other asymmetrical bolalipids that derived from
20
21 archaeobacteria can also form interdigitated monolayer membranes.⁴⁷
22
23
24
25
26
27



28
29
30
31
32
33
34
35
36
37
38
39
40
41
42
43
44
45 **Figure 6.** Left: Scheme of a lamellar phase consisting of interdigitated asymmetrical bolalipid
46 molecules in a monolayer arrangement with a tilt of 30° of the bolalipid molecules relative to the
47 layer normal. This tilt is possibly caused by steric reasons to optimize packing for the phenyl
48 rings. Right: CPK-model of seven PC-C17pPhC17-OH molecules in a monolayer arrangement.
49
50

51
52 In the wide angle X-ray scattering (WAXS) region, 6 sharp reflections appear which we could
53 not index so far. The reflections indicate a well ordered almost crystalline-like packing of the
54 alkyl chains. The WAXS-pattern could reflect a superposition of two individually scattering
55
56
57
58
59
60

1
2
3 triclinic lattices (with three reflections for each lattice). More detailed studies on the indexing
4
5 will be the focus of future work.
6
7

8 At 58 °C a change in scattering in the SAXS region occurs, only three reflections with much
9
10 higher intensities are observable above the DSC transition. The position of the first order
11
12 reflection is shifted to $s = 0.158 \text{ nm}^{-1}$ at 70 °C ($d = 6.32 \text{ nm}$). A further increase in temperature
13
14 leads to a further shift in the position of s_1 to $s = 0.120 \text{ nm}^{-1}$ ($d = 8.33 \text{ nm}$) at 100 °C indicating
15
16 an increase in lamellar repeat spacing probably due to an increase in water layer thickness.
17
18

19
20 In the WAXS region, heating to 58 °C, above the T_m observed in the DSC, a drastic change of
21
22 the scattering pattern occurs, as now, essentially only one reflection remains (see also Figure
23
24 S10). The maximum of the peak is located at $s_1 = 2.348 \text{ nm}^{-1}$. Closer inspection shows that it
25
26 might be superimposed on a broad reflection at $s_2 = 2.458 \text{ nm}^{-1}$. This would indicate an L_β chain
27
28 packing mode. The FTIR spectra taken at temperatures above 58 °C showed that some disor-
29
30 dering of the chains has already set in as the CH_2 -deformation band has shifted and the frequency
31
32 of the CH_2 -stretching bands have also increased slightly (see above). It is therefore likely that the
33
34 chains are tilted and the alkyl chain segments become rotationally disordered above 58 °C.
35
36
37
38

39 In contrast to DSC or FT-IR measurements, the sample used for X-ray scattering experiments
40
41 could be heated to high temperature as the capillary was sealed. Therefore, the "melting
42
43 temperature" of the lamellar monolayer phase could be determined. At a temperature above
44
45 120 °C, the chains become finally disordered and a fluid lamellar phase is formed as indicated by
46
47 the broad halo in the WAXS region caused by the scattering of disordered chains. The SAXS
48
49 reflections at high temperature phase indicate the presence of a larger repeat distance ($s =$
50
51 0.125 nm^{-1} , $d = 8.00 \text{ nm}$) though only two SAXS reflections are present and a lamellar lattice
52
53 cannot be reliably indexed. This would indicate that the decrease in monolayer thickness due to
54
55
56
57
58
59
60

1
2
3 the fluidization of the chains is overcompensated by an increase in water layer thickness.
4

5 For the interdigitated monolayer membrane of the previously investigated bolalipid
6 DMAPPC-C32-OH with unmodified but effectively shorter chain we also found that the
7 transition into the fluid lamellar phase occurred at very high temperature above 100 °C.²⁴ For a
8 similar compound with only 22 CH₂-groups (PC-C22-OH) a transition into the fluid lamellar
9 monolayer phase at a temperature of 80 °C was found.⁴⁶ Therefore, it is clear that the transition
10 into a fluid monolayer phase is dependent on the chain length. In the case of PC-C17pPhC17-OH
11 the phenyl ring in the middle of the chain increases effectively the chain length, but on the other
12 hand leads to a perturbation of the chain packing. Thus the observed "melting" temperature is
13 somewhat lower than expected from the overall chain length but still higher than the other
14 compounds with shorter chains.
15
16
17
18
19
20
21
22
23
24
25
26
27
28

29 The additional phenyl ring in the middle part of the alkyl chain of both bolalipids could be
30 capable for pi stacking that possibly increases the interaction of different bola molecules.
31 However, these interactions are short-ranged and further depend on the relative orientations of
32 the benzene rings interacting with each other. This orientation is in turn basically determined by
33 steric requirements of the PC headgroup area in comparison to the cross-sectional area of the
34 single alkyl chain, which lead to a helical arrangement of symmetrical bola molecules within the
35 nanofibers¹⁰ and, hence, the phenyl rings cannot come into a close contact for constructive pi
36 stacking. For the asymmetrical bolalipids the pi stacking could become more likely since the
37 alkyl chains can get into a closer contact due the smaller hydroxy headgroup and the resulting
38 interdigitated arrangement of the bolalipid molecules within the monolayer (see CPK-model in
39 Figure 6 right part). However, the contribution of pi stacking to the strength of intermolecular
40 interaction is, in our view, small and the self-assembly of the bolalipids in lamellar aggregates
41
42
43
44
45
46
47
48
49
50
51
52
53
54
55
56
57
58
59
60

1
2
3 and also nanofibers is mainly driven by hydrophobic (van-der-Waals) interactions of the long
4
5
6 alkyl chain.
7

8 *Packing parameter P:*
9

10 An explanation for the different aggregation behavior of both bolalipids, which is obviously
11 related to the headgroups' asymmetry, could probably be found applying the packing parameter
12 (*P*). This parameter was introduced by Israelachvili^{48,49} to predict the aggregation behavior of
13 classical monopolar amphiphiles in water. The adaptation of this geometrical approach from
14 *monopolar* to *bipolar* lipids is problematic, since the single-chain bolalipids mostly have a
15 stretched (all-*trans*) alkyl chain conformation and, hence, two “*separated*” headgroups rather
16 than a *U-shaped* conformation bearing the two headgroups in a close contact. However, in a
17 recent publication we applied this concept for bipolar lipids with a single unmodified C32-alkyl
18 chain and symmetrical headgroups of different size. We could show that nanofibers are the stable
19 aggregate form if the values of *P* are in the range between 0.28 and 0.41.¹³ If *P* exceeds a value
20 of 0.41, the formation of lamellar or sheet-like aggregates is preferred. In the present case, the
21 symmetrical PC-C17pPhC17-PC has a value of *P* = 0.40 and the asymmetrical PC-C17pPhC17-
22 OH a value of *P* = 0.57 (see Figure S11, Table S4 and SI for further details). These calculated *P*
23 values could hence be an explanation for the different aggregation behavior of both bolalipid in
24 water although this value is only of minor significance for bipolar amphiphiles (see SI).
25
26
27
28
29
30
31
32
33
34
35
36
37
38
39
40
41
42
43
44
45

46 **Mixing behavior with classical phospholipids**

47
48
49 *PC-C17pPhC17-PC with DPPC and DSPC:*
50

51 For the mixing experiments of both bolalipids with bilayer forming phospholipids we chose
52 the double-chain phospholipids DPPC and DSPC. Unmodified bolalipids, such as PC-C32-PC,
53 did not incorporate into phospholipid bilayers of, *e.g.*, DPPC, 1,2-dimyristoyl-*sn*-glycero-3-
54
55
56
57
58
59
60

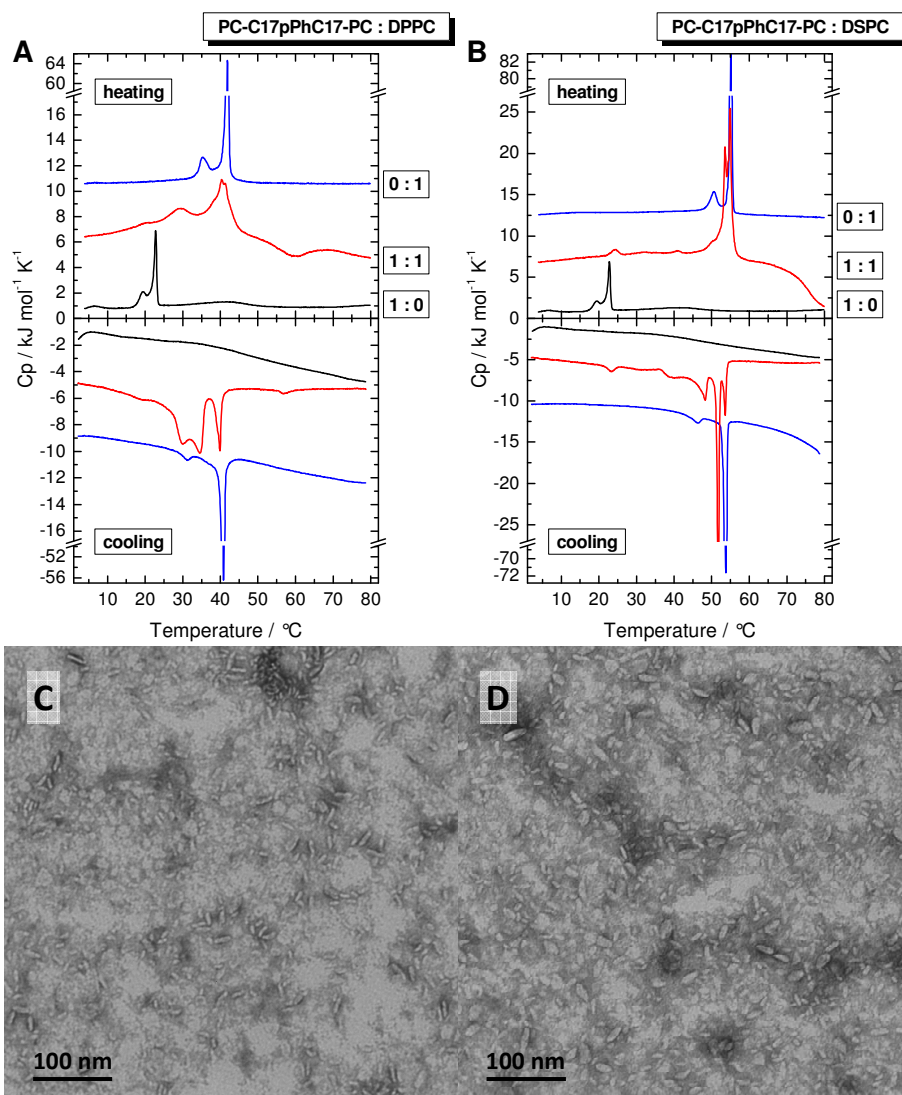
1
2
3 phosphocholine (DMPC), or 1-palmitoyl-2-oleoyl-*sn*-glycero-3-phosphocholine (POPC) due to
4
5 packing frustration caused by the larger space requirement of the PC headgroup of PC-C32-PC
6
7 in comparison to the small cross-sectional area of the alkyl chain.⁵⁰ The additional phenylene
8
9 ring in the middle part of the alkyl chain of both bolalipids investigated in this work increases the
10
11 volume of the hydrocarbon chain, which could possibly improve the miscibility with
12
13 phospholipids and, at best, result in a stabilized bilayer membrane.
14
15

16
17 We first investigated the thermotropic behavior of aqueous suspensions of equimolar mixtures
18
19 of the symmetrical PC-C17pPhC17-PC with DPPC (Figure 7A) and DSPC (Figure 7B). In the
20
21 case of pure DPPC and DSPC, the two well-known endothermic transitions are observed in the
22
23 thermogram: the pre-transition from L_{β^-} to the P_{β^-} -phase (ripple phase) and the main transition at
24
25 41.9 °C (DPPC) and 54.9 °C (DSPC) to the L_{α} -phase. The pure PC-C17pPhC17-PC shows a
26
27 fiber-micelle-transition at 22.8 °C. In an equimolar mixture of PC-C17pPhC17-PC with DPPC
28
29 the DSC heating scan (Figure 7A) show two endothermic transitions between 2 °C and 80 °C: a
30
31 broad transition at $T = 29\text{--}30$ °C and a second one slightly below the DPPC main transition with
32
33 a splitting (40.4 °C, 41.3 °C). The corresponding cooling curve shows three peaks at 39.9 °C,
34
35 34.6 °C, and 30.0 °C, whereas the cooling scan of the pure bolalipid shows no transition due to
36
37 the slow kinetics for the reformation of the nanofibers as already described above.
38
39
40
41
42
43

44 Similar results were found for the equimolar mixture of PC-C17pPhC17-PC with the longer
45
46 chain DSPC. In the DSC heating scan (Figure 7B) we observe two large endothermic transitions
47
48 at 53.5 °C and 54.9 °C together with two small peaks at 24.2 °C and 41.0 °C. The corresponding
49
50 cooling scan reveals several transition peaks, the most distinctive ones at 53.6 °C, 51.8 °C, and
51
52 48.3 °C.
53
54

55 In addition, the DSC heating scan of the DPPC-mixture shows a reproducible, exothermic
56
57
58
59
60

1
2
3 transition peak at about 60 °C. For the corresponding DSPC-mixture only a decrease in the heat
4
5 capacity beginning at 70 °C is seen. The origin of this effect remains unclear at this time, but it is
6
7 conceivable that a metastable state is reached after the main transition, which further transforms
8
9 within the timescale of the DSC experiment (heating rate = 60 K h⁻¹) into a thermodynamically
10
11 stable state indicated by this exothermic transition. The same effect was found earlier for a mix-
12
13 ture of DPPC with PC-C32-10,10'-Me-PC – a bolalipid with two methyl groups in the chain.¹³
14
15
16
17



18
19
20
21
22
23
24
25
26
27
28
29
30
31
32
33
34
35
36
37
38
39
40
41
42
43
44
45
46
47
48
49
50
51
52
53
54
55
56
57
58
59
60
Figure 7. A,B: DSC heating and cooling curves of equimolar mixtures ($c = 3$ mM) of PC-C17pPhC17-PC with DPPC (A) and DSPC (B) in phosphate buffer solution (10 mM, pH = 7.4). DSC curves of pure compounds are presented for comparison. The curves are shifted vertically

1
2
3 for clarity. C,D: TEM images of equimolar mixtures ($c = 60 \mu\text{M}$) of PC-C17pPhC17-PC with (C)
4 DPPC and (D) DSPC in phosphate buffer (10 mM, pH = 7.4). The samples were prepared at
5 room temperature and negatively stained with uranyl acetate.
6
7

8
9 To get an idea about the shape of the aggregates formed in aqueous suspension TEM images
10 were recorded from negatively stained samples. All samples were prepared at room temperature,
11 *i.e.*, below the transitions observed in DSC. The images are shown in Figure 7C,D. In both cases,
12
13 no closed lipid vesicles (liposomes) can be observed as found for pure DPPC and DSPC in
14 aqueous suspension. Instead, small elongated micelles and small bilayer fragments are present.
15
16 These aggregates have a size of about 20–30 nm in length and in the case of bilayer fragments
17 they are either oriented parallel or perpendicular to the surface of the grid. We can only speculate
18 about the composition of these mixed lipid aggregates, but it seems clear from the images and
19 also from the DSC curves that a partial demixing occurs. The elongated micelles contain
20 probably mostly bolalipids with some phospholipids and the bilayer disks contain some
21 bolalipids probably enriched at the rim of the phospholipid bilayer fragments.
22
23
24
25
26
27
28
29
30
31
32
33

34 Based on the DSC data, the TEM images, and the fact that both bolalipid : phospholipid
35 mixtures are clear and transparent solutions (without the use of sonication) we can conclude that
36 we indeed have a partial miscibility of both components, which is in contrast to mixtures of the
37 unmodified PC-C32-PC with DPPC. In the latter case, EM images showed a coexistence of long
38 PC-C32-PC nanofibers and DPPC vesicles.⁵⁰
39
40
41
42
43
44
45
46

47 *PC-C17pPhC17-OH with DPPC:*

48
49 In the second series of mixing experiments we used the asymmetrical PC-C17pPhC17-OH
50 together with DPPC. Since PC-C17pPhC17-OH forms lamellar aggregates by itself, the possi-
51 bility exists that this asymmetrical bolalipid can be incorporated into DPPC bilayers leading to a
52 stabilization of the DPPC lipid membranes. The temperature dependent aggregation behavior of
53
54
55
56
57
58
59
60

1
2
3 PC-C17pPhC17-OH : DPPC mixtures at different molar ratios was again investigated by
4 calorimetric measurements (see Figure 8).
5
6

7
8 The DSC heating scans in Figure 8A show that T_m of DPPC at 41.9 °C is not affected by an
9 increasing amount of the asymmetrical bolalipid. The transition peak of PC-C17pPhC17-OH is
10 slightly shifted to higher temperatures (by 1.2 K to 54.6 °C) in mixtures with DPPC. In addition,
11 a second endothermic transition occurs at 57.8 °C. Both transition peaks stay at the same temper-
12 ature independent of the mixing ratio. In the cooling scans only two peaks are observed (Figure
13 8B): T_m of DPPC is again not influenced by the bolalipid and the PC-C17pPhC17-OH transition
14 is shifted to slightly higher temperatures by 1.3 K compared to the pure bolalipid but in this case
15 no additional transition is observed. Again, both transitions stay at the same temperature for each
16 molar ratio investigated, only that the relative peak areas change according to the mixing ratio.
17
18
19
20
21
22
23
24
25
26
27
28

29 The DSC curves clearly indicate that the asymmetrical bolalipid PC-C17pPhC17-OH cannot
30 be incorporated into DPPC bilayer membranes. These two lipids seem to be almost completely
31 immiscible despite the fact that both form lamellar phases, DPPC a bilayer phase and PC-
32 C17pPhC17-OH a monolayer lamellar phase. The small increase in the main transition
33 temperature of PC-C17pPhC17-OH in its mixtures with DPPC indicates that possibly a small
34 amount of DPPC can be inserted in the lamellar monolayer structures of the bolalipid. Likewise
35 the slight broadening of the main transition of DPPC indicates some perturbation of the packing
36 due to incorporation of the bolalipid into the bilayer membranes.
37
38
39
40
41
42
43
44
45
46
47
48
49
50
51
52
53
54
55
56
57
58
59
60

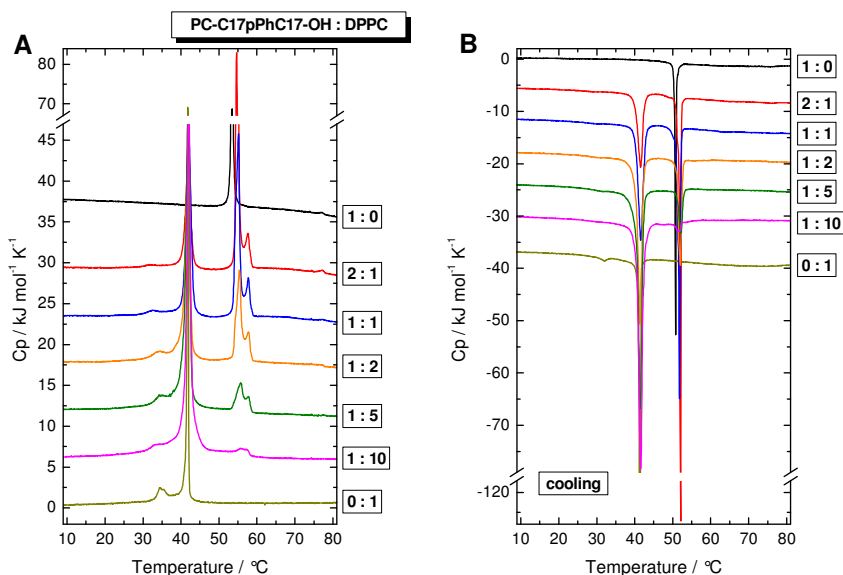


Figure 8. DSC curves of 3 mM suspensions of PC-C17pPhC17-OH : DPPC mixtures in phosphate buffer solution (10 mM, pH = 7.4) with different molar ratios: (A) heating, (B) cooling. The heating/cooling rate was 20 K h^{-1} . The curves are shifted vertically for clarity.

These findings are supported by TEM images (Figure 9) of uranyl acetate stained suspensions of PC-C17pPhC17-OH : DPPC mixtures that show the presence of two different aggregate types: on the one hand closed bilayer vesicles formed of DPPC and on the other hand large lamellar aggregates composed of the asymmetrical bolalipid. The immiscibility is probably due to the fact that PC-C17pPhC17-OH forms a very stable monolayer lamellar phase, which becomes fluid only at very high temperature above $120 \text{ }^{\circ}\text{C}$ (see above). This is energetically favored over the incorporation into DPPC bilayer membranes as in this case the formation of void volume cannot be avoided when PC-C17pPhC17-OH is in a stretched conformation. This is due to packing problems caused by the large space requirement of the PC headgroup of PC-C17pPhC17-OH compared to the small cross-sectional area of the alkyl chain. Thus, the PC-C17pPhC17-OH prefers to self-assemble into separate lamellar aggregates, where the alkyl chain of the bolalipid can get in very close contact.

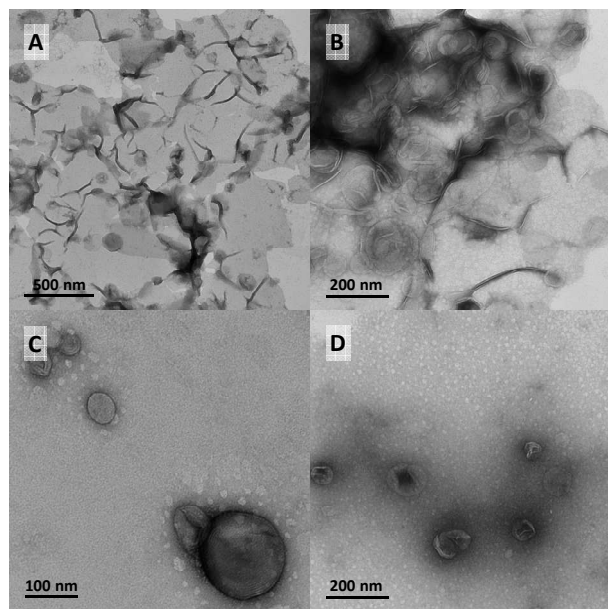


Figure 9. TEM images of PC-C17pPhC17-OH:DPPC mixtures ($c = 60 \mu\text{M}$ in phosphate buffer solution 10 mM, pH = 7.4) with different molar ratios: A) 2:1, B) 1:1, C) 1:5 and D) 1:10. The samples were prepared at room temperature and stained with uranyl acetate solution.

CONCLUSIONS

Two single-chain phenylene-modified bolalipids with either two phosphocholine headgroups resulting in a symmetrical example (PC-C17pPhC17-PC) or a phosphocholine and a hydroxy headgroup leading to the asymmetrical counterpart (PC-C17pPhC17-OH) were synthesized using a stepwise Sonogashira cross-coupling reaction of dibromo benzene derivatives with various, orthogonally protected alkynols as key step.

The aggregation behavior of both bolalipids in aqueous suspension as a function of temperature showed that depending on the headgroup asymmetry, nanofibers or lamellar aggregates are formed: The symmetrical PC-C17pPhC17-PC self-assembles into nanofibers with a diameter of 5.7 nm corresponding to the length of bolalipid molecule. Physical cross-linking and entanglements of the fibers lead to a gelation of water. However, this hydrogel is less stable compared to a hydrogel composed of unmodified bolalipids, *e.g.*, PC-C32-PC, due to the

1
2
3 additional phenyl ring within the alkyl chain. An increase in temperature leads to the reversible
4
5 transformation of the nanofibers into small elongated micelles.
6
7

8 The asymmetrical PC-C17pPhC17-OH self-assembles in aqueous suspension into large
9
10 lamellar structures. The thickness of the lamellae is 6.66 nm indicating a monolayer of molecules
11
12 with interdigitated alkyl chains. The alkyl chains are in an all-*trans* conformation, closely packed
13
14 and possibly tilted relative to the layer normal. An increase in temperature above 58 °C causes a
15
16 change in the packing mode and the chains become probably rotationally disordered however
17
18 retaining their all-*trans* conformation up to very high temperatures of about 120 °C. Above this
19
20 temperature a melting of the alkyl chains into liquid-crystalline phases occurs.
21
22
23

24 The mixing behavior of these novel phenylene-modified bolalipids with bilayer forming
25
26 phospholipids, *e.g.*, DPPC and DSPC, was studied by DSC and by TEM. We observed a
27
28 completely different mixing behavior of both bolalipids depending on the headgroup asymmetry:
29
30 The symmetrical PC-C17pPhC17-PC is partially miscible with DPPC and DSPC, respectively,
31
32 however, closed lipid vesicles are not observed and bilayer fragments as well as elongated
33
34 micelles are formed instead. The main phase transitions of DPPC or DSPC are slightly
35
36 broadened but not significantly shifted indicating that no stabilization effect of the bilayers by
37
38 the bolalipid occurs. The asymmetrical PC-C17pPhC17-OH shows almost complete immiscibi-
39
40 lity with DPPC at all DPPC : PC-C17pPhC17-OH ratios despite the fact that both components
41
42 self-assemble in aqueous suspensions in lamellar structures. This is indicated by the DSC scans
43
44 showing two independent endothermic transitions that belong to the pure compounds and by the
45
46 TEM images, where two types of aggregates, closed vesicles of DPPC and large lamellae of the
47
48 bolalipid are seen. The results show that a delicate balance between steric requirements of the
49
50 headgroups and alkyl chains and intermolecular interactions in these long-chain compounds
51
52
53
54
55
56
57
58
59
60

1
2
3 leads to quite unexpected mixing behavior with classical phospholipids forming lipid bilayer
4
5 phases.
6
7

8 ASSOCIATED CONTENT

9
10
11
12 **Supporting Information.** Synthetic procedures, analytical data, ESI-MS, ^1H -, ^{13}C -NMR, and
13
14 HRMS spectra of prepared compounds, additional DSC, FTIR, and TEM measurements, further
15
16 SANS and X-ray scattering data. This material is available free of charge via the Internet at
17
18 <http://pubs.acs.org>.
19
20
21

22 AUTHOR INFORMATION

23 **Corresponding Author**

24
25
26
27 *simon.drescher@pharmazie.uni-halle.de, phone: +49-345-5525196, fax: +49-345-5527026.
28
29
30

31 **Author Contributions**

32
33
34 The manuscript was written by contributions of all authors. All authors have given approval to
35
36 the final version of the manuscript.
37
38

39 ACKNOWLEDGMENT

40
41
42 This work was financially supported by grants (project Bl 182/19-3 to S.D., A.M., and A.B.) and
43
44 by grants within to Forschergruppe FOR 1145 (to B.-D.L. and A.B.) from the Deutsche
45
46 Forschungsgemeinschaft (DFG). This research project has also been supported by the European
47
48 Commission under the 7th Framework Programmes through the 'Research Infrastructures' action
49
50 of the 'Capacities Programme' Contact No: CP-CSA_INFRA-2008-1.1.1 Number 226507-
51
52 NMI3. The support of Dr Gerd Hause (Biocenter, MLU Halle-Wittenberg) by providing us
53
54 access to the electron microscope facility is greatly appreciated. Finally, S.D. thanks Prof Andrea
55
56
57
58
59
60

1
2
3 Sinz and Dr Christian Ihling (Department of Pharmaceutical Chemistry and Bioanalytics, MLU
4
5 Halle-Wittenberg) for the high resolution mass spectrometry analysis.
6
7

8
9 REFERENCES

- 10
11
12 (1) Fuhrhop, J.-H.; Wang, T. Bolaamphiphiles. *Chem. Rev.* **2004**, *104*, 2901-2937.
13
14 (2) Langworthy, T. A. Long-chain diglycerol tetraethers from *Thermoplasma acidophilum*.
15
16 *Biochim. Biophys. Acta, Lipids Lipid Metab.* **1977**, *487*, 37-50.
17
18 (3) De Rosa, M.; Esposito, E.; Gambacorta, A.; Nicolaus, B.; Bu'Lock, J. D. Effects of
19
20 temperature on ether lipid composition of *Caldariella acidophila*. *Phytochemistry* **1980**, *19*, 827-
21
22 831.
23
24 (4) Gambacorta, A.; Gliozzi, A.; Rosa, M. Archaeal lipids and their biotechnological
25
26 applications. *World J. Microb. Biot.* **1995**, *11*, 115-131.
27
28 (5) Estroff, L. a.; Hamilton, A. D. Water gelation by small organic molecules. *Chem. Rev.* **2004**,
29
30 *104*, 1201-1218.
31
32 (6) Benvegna, T.; Brard, M.; Plusquellec, D. Archaeobacteria bipolar lipid analogues: structure,
33
34 synthesis and lyotropic properties. *Curr. Opin. Colloid Interface Sci.* **2004**, *8*, 469-479.
35
36 (7) Benvegna, T.; Lemiègre, L.; Cammas-Marion, S. Archaeal Lipids: Innovative Materials for
37
38 Biotechnological Applications. *Eur. J. Org. Chem.* **2008**, *2008*, 4725-4744.
39
40 (8) Yan, Y.; Lu, T.; Huang, J. Recent advances in the mixed systems of bolaamphiphiles and
41
42 oppositely charged conventional surfactants. *J. Colloid Interf. Sci.* **2009**, *337*, 1-10.
43
44 (9) Chong, P. L.-G. Archaeobacterial bipolar tetraether lipids: Physico-chemical and membrane
45
46 properties. *Chem. Phys. Lipids* **2010**, *163*, 253-265.
47
48 (10) Köhler, K.; Förster, G.; Hauser, A.; Dobner, B.; Heiser, U. F.; Ziethe, F.; Richter, W.;
49
50 Steiniger, F.; Drechsler, M.; Stettin, H.; Blume, A. Temperature-dependent behavior of a
51
52
53
54
55
56
57
58
59
60

1
2
3 symmetric long-chain bolaamphiphile with phosphocholine headgroups in water: from hydrogel
4
5 to nanoparticles. *J. Am. Chem. Soc.* **2004**, *126*, 16804-16813.

7
8 (11) Meister, A.; Drescher, S.; Mey, I.; Wahab, M.; Graf, G.; Garamus, V. M.; Hause, G.; Mögel,
9
10 H.-J.; Janshoff, A.; Dobner, B.; Blume, A. Helical nanofibers of self-assembled bipolar
11
12 phospholipids as template for gold nanoparticles. *J. Phys. Chem. B* **2008**, *112*, 4506-4511.

13
14 (12) Wahab, M.; Schiller, P.; Schmidt, R.; Moegel, H. J. Monte Carlo Study of the Self-Assembly
15
16 of Achiral Bolaform Amphiphiles into Helical Nanofibers. *Langmuir* **2010**, *26*, 2979-2982.

17
18 (13) Blume, A.; Drescher, S.; Meister, A.; Graf, G.; Dobner, B. Tuning the Aggregation
19
20 Behaviour of Single-Chain Bolaphospholipids in Aqueous Suspension: From Nanoparticles to
21
22 Nanofibres to Lamellar Phases. *Faraday Disc.* **2013**, *161*, 193-213.

23
24 (14) Drescher, S.; Meister, A.; Blume, A.; Karlsson, G.; Almgren, M.; Dobner, B. General
25
26 synthesis and aggregation behaviour of a series of single-chain 1, ω -bis(phosphocholines). *Chem.*
27
28 *Eur. J.* **2007**, *13*, 5300-5307.

29
30 (15) Graf, G.; Drescher, S.; Meister, A.; Garamus, V. M.; Dobner, B.; Blume, A. Bolalipid fiber
31
32 aggregation can be modulated by the introduction of sulfur atoms into the spacer chains. *J. Coll.*
33
34 *Interf. Sci.* **2013**, *393*, 143-150.

35
36 (16) Meister, A.; Bastrop, M.; Koschoreck, S.; Garamus, V. M.; Sinemus, T.; Hempel, G.;
37
38 Drescher, S.; Dobner, B.; Richtering, W.; Huber, K.; Blume, A. Structure-property relationship in
39
40 stimulus-responsive bolaamphiphile hydrogels. *Langmuir* **2007**, *23*, 7715-7723.

41
42 (17) Meister, A.; Drescher, S.; Karlsson, G.; Hause, G.; Baumeister, U.; Hempel, G.; Garamus, V.
43
44 M.; Dobner, B.; Blume, A. Formation of square lamellae by self-assembly of long-chain
45
46 bolaphospholipids in water. *Soft Matter* **2010**, *6*, 1317-1324.

- 1
2
3 (18) Meister, A.; Drescher, S.; Garamus, V. M.; Karlsson, G.; Graf, G.; Dobner, B.; Blume, A.
4
5 Temperature-dependent self-assembly and mixing behavior of symmetrical single-chain
6
7 bolaamphiphiles. *Langmuir* **2008**, *24*, 6238-6246.
8
9
10 (19) Fuhrhop, J.-H.; Spiroski, D.; Boettcher, C. Molecular monolayer rods and tubules made of
11
12 α -(L-lysine), ω -(amino) bolaamphiphiles. *J. Am. Chem. Soc.* **1993**, *115*, 1600-1601.
13
14
15 (20) Masuda, M.; Shimizu, T. Lipid nanotubes and microtubes: experimental evidence for
16
17 unsymmetrical monolayer membrane formation from unsymmetrical bolaamphiphiles. *Langmuir*
18
19 **2004**, *20*, 5969-5977.
20
21
22 (21) Kameta, N.; Masuda, M.; Minamikawa, H.; Mishima, Y.; Yamashita, I.; Shimizu, T.
23
24 Functionalizable Organic Nanochannels Based on Lipid Nanotubes: Encapsulation and
25
26 nanofluidic Behavior of Biomacromolecules. *Chem. Mater.* **2007**, *19*, 3553-3560.
27
28
29 (22) Kameta, N.; Masuda, M.; Minamikawa, H.; Shimizu, T. Self-Assembly and Thermal Phase
30
31 Transition Behavior of Unsymmetrical Bolaamphiphiles Having Glucose- and Amino-
32
33 Hydrophilic Headgroups. *Langmuir* **2007**, *23*, 4634-4641.
34
35
36 (23) Masuda, M.; Shimizu, T. Multilayer structure of an unsymmetrical monolayer lipid
37
38 membrane with a 'head-to-tail' interface. *Chem. Commun.* **2001**, 2442-2443.
39
40
41 (24) Graf, G.; Drescher, S.; Meister, A.; Garamus, V. M.; Dobner, B.; Blume, A. Tuning the
42
43 Aggregation Behaviour of Single-Chain Bolaamphiphiles in Aqueous Suspension by Changes in
44
45 Headgroup Asymmetry. *Soft Matter* **2013**, *9*, 9562-9571.
46
47
48 (25) Gabriel, J. L.; Chong, P. L. Molecular modeling of archaebacterial bipolar tetraether lipid
49
50 membranes. *Chem. Phys. Lipids* **2000**, *105*, 193-200.
51
52
53 (26) Gu, Q.; Zou, A.; Yuan, C.; Guo, R. Effects of a bolaamphiphile on the structure of
54
55 phosphatidylcholine liposomes. *J. Colloid Interf. Sci.* **2003**, *266*, 442-447.
56
57
58
59
60

- 1
2
3
4 (27) Fuhrhop, J. H.; Liman, U.; Koesling, V. A Macrocyclic Tetraether Bolaamphiphile and an
5
6 Oligoamino α,ω -Dicarboxylate Combine To Form Monolayered, Porous Vesicle Membranes,
7
8 Which Are Reversibly Sealed by EDTA and Other Bulky Anions. *J. Am. Chem. Soc.* **1988**, *110*,
9
10 6840-6845.
11
12 (28) Moss, R. A.; Li, G.; Li, J.-M. Enhanced Dynamic Stability of Macrocyclic and
13
14 Bolaamphiphilic Macrocyclic Lipids in Liposomes. *J. Am. Chem. Soc.* **1994**, *116*, 805-806.
15
16 (29) Sprott, G. D.; Tolson, D. L.; Patel, G. B. Archaeosomes as novel antigen delivery systems.
17
18 *FEMS Microbiol. Lett.* **1997**, *154*, 17-22.
19
20 (30) Benvegna, T.; Réthoré, G.; Brard, M.; Richter, W.; Plusquellec, D. Archaeosomes based on
21
22 novel synthetic tetraether-type lipids for the development of oral delivery systems. *Chem.*
23
24 *Commun.* **2005**, 5536-5538.
25
26 (31) Jacquemet, A.; Barbeau, J.; Lemiègre, L.; Benvegna, T. Archaeal tetraether bipolar lipids:
27
28 Structures, functions and applications. *Biochimie* **2009**, *91*, 711-717.
29
30 (32) Grinberg, S.; Kipnis, N.; Linder, C.; Kolot, V.; Heldman, E. Asymmetric bolaamphiphiles
31
32 from vernonia oil designed for drug delivery. *Eur. J. Lipid Sci. Technol.* **2010**, *112*, 137-151.
33
34 (33) Nuraje, N.; Bai, H.; Su, K. Bolaamphiphilic molecules: Assembly and applications.
35
36 *Progress in Polymer Science* **2013**, *38*, 302-343.
37
38 (34) Philosof-Mazor, L.; Dakwar, G. R.; Popov, M.; Kolusheva, S.; Shames, A.; Linder, C.;
39
40 Greenberg, S.; Heldman, E.; Stepensky, D.; Jelinek, R. Bolaamphiphilic vesicles encapsulating
41
42 iron oxide nanoparticles: New vehicles for magnetically targeted drug delivery. *Int. J. Pharm.*
43
44 **2013**, *450*, 241-249.
45
46 (35) Rosta, L. Cold neutron research facility at the Budapest Neutron Centre. *Appl. Phys. A* **2002**,
47
48 *74*, 292-294.
49
50
51
52
53
54
55
56
57
58
59
60

- 1
2
3
4 (36) Drescher, S.; Becker, S.; Dobner, B.; Blume, A. Bis-Sonogashira Cross-Coupling: An
5
6 Expeditious Approach towards Long-Chain, Phenylene-Modified 1, ω -Diols. *RSC Adv.* **2012**, *2*,
7
8 4052-4054.
9
- 10 (37) Drescher, S.; Sonnenberger, S.; Meister, A.; Blume, A.; Dobner, B. Synthesis and
11
12 Aggregation Behaviour of Symmetrical Phenylene/Biphenylene-modified Bolaamphiphiles.
13
14 *Monatsh. Chem.* **2012**, *143*, 1533-1543.
15
- 16 (38) Mantsch, H. H.; McElhaney, R. N. Phospholipid phase transitions in model and biological
17
18 membranes as studied by infrared spectroscopy. *Chem. Phys. Lipids* **1991**, *57*, 213-226.
19
- 20 (39) Mendelsohn, R.; Moore, D. J. Vibrational spectroscopic studies of lipid domains in
21
22 biomembranes and model systems. *Chem. Phys. Lipids* **1998**, *96*, 141-157.
23
- 24 (40) Snyder, R. G. Vibrational spectra of crystalline n-paraffins II. Intermolecular effects. *J. Mol.*
25
26 *Spectrosc.* **1961**, *7*, 116-144.
27
- 28 (41) Snyder, R. G. Vibrational correlation splitting and chain packing for the crystalline alkanes.
29
30 *J. Chem. Phys.* **1979**, *71*, 3229-3235.
31
- 32 (42) Lewis, R. N. A. H.; McElhaney, R. N. Studies of Mixed-Chain Diacyl Phosphatidylcholines
33
34 with Highly Asymmetric Acyl Chains: A Fourier Transform Infrared Spectroscopic Study of
35
36 Interfacial Hydration and Hydrocarbon Chain Packing in the Mixed Interdigitated Gel Phase.
37
38 *Biophys. J.* **1993**, *65*, 1866-1877.
39
- 40 (43) Wong, P. T. T. Pressure-induced Correlation Field Splitting of Vibrational Modes: Structural
41
42 and Dynamic Properties in Lipid Bilayers and Biomembranes. *Biophys. J.* **1994**, *66*, 1505-1514.
43
- 44 (44) Glatter, O. A New Method for the Evaluation of Small-Angle Scattering Data. *J. Appl.*
45
46 *Cryst.* **1977**, *10*, 415-421.
47
48
49
50
51
52
53
54
55
56
57
58
59
60

- 1
2
3 (45) Pedersen, J. S. Analysis of small-angle scattering data from colloids and polymer solutions:
4 modeling and least-squares fitting. *Adv. Colloid Interf. Sci.* **1997**, *70*, 171-210.
5
6
7
8 (46) Pohle, W.; Selle, C.; Rettig, W.; Heiser, U.; Dobner, B.; Wartewig, S. Phase transitions and
9 hydrogen bonding in a bipolar phosphocholine evidenced by calorimetry and vibrational
10 spectroscopy. *Arch. Biochem. Biophys.* **2001**, *396*, 151-161.
11
12
13 (47) Gliozzi, A., In *Handbook of Nonmedical Applications of Liposomes*, Barenholz, Y.; Lasic,
14 D. D., Eds. CRC Press: Boca Raton, New York/London/Tokyo, 1996; Vol. II, p 329.
15
16
17 (48) Israelachvili, J. N.; Marcelja, S.; Horn, R. G. Physical principles of membrane organisation.
18
19
20
21
22 *Quart. Rev. Biophys.* **1980**, *13*, 121-200.
23
24 (49) Israelachvili, J. N., *Intermolecular and Surface Forces*. 3rd ed.; Academic Press:
25 Burlington, 2011.
26
27
28 (50) Meister, A.; Köhler, K.; Drescher, S.; Dobner, B.; Karlsson, G.; Edwards, K.; Hause, G.;
29 Blume, A. Mixing behaviour of a symmetrical single-chain bolaamphiphile with phospholipids.
30
31
32
33
34 *Soft Matter* **2007**, *3*, 1025-1031.
35
36
37
38
39
40
41
42
43
44
45
46
47
48
49
50
51
52
53
54
55
56
57
58
59
60

1
2
3
4
5
6
7
8
9
10
11
12
13
14
15
16
17
18
19
20
21
22
23
24
25
26
27
28
29
30
31
32
33
34
35
36
37
38
39
40
41
42
43
44
45
46
47
48
49
50
51
52
53
54
55
56
57
58
59
60

